Segmentation of Human Upper Airway Using a Level Set Based Deformable Model

Si Yong Yeo[a], Xianghua Xie[b], Igor Sazonov[a] and Perumal Nithiarasu[a]

[a]School of Engineering, Swansea University, Swansea SA2 8PP, U.K.
[b]Department of Computer Science, Swansea University, Swansea SA2 8PP, U.K.
{465186, X.Xie, I.Sazonov, P.Nithiarasu} @swansea.ac.uk

Abstract. In this paper, we present a preliminary study on segmenting a human upper airway from a 3D CT scan using a level set based deformable surface model. The human upper airway has a very complex geometry and its topology may vary from individual to individual. Accurate 3D geometry reconstruction is essential in understanding airway disease and a prerequisite for patient-specific computational fluid dynamics analysis. The proposed method uses a hypothesized dynamic interaction force between the deformable surface and object boundaries which can greatly improve the deformable model performance in acquiring complex geometries, boundary concavities, and in dealing with weak image edges. The results show that the proposed deformable model can be used to efficiently segment complex and compact structures such as the nasal cavity from a 3D image dataset.

1 Introduction

The human upper airway is the primary conduit for passage of air to the respiratory system. There are several airway related problems which have been recently recognised to affect a significant portion of the human population. The nasal cavity (part of the upper airway) which conditions and filters the inspired air forms the uppermost part of the human airway system. Numerous studies, for example [1, 2], on the nasal cavity have shown that the function and airflow of the nasal cavity are likely to be associated with some airway diseases (for example, sleep apnoea), and are important in the treatment of such diseases. Thus, knowledge on the function and airflow of the nasal cavity will help in understanding the human airway diseases and will result in the development of efficient treatment methods.

The complex geometry and narrow passages of the nasal cavity have made detailed experimental studies of the nasal airflow challenging. It is also worth noting that its topology may vary from individual to individual, which makes it difficult for atlas based techniques. Recently, some numerical models, e.g. [3–6], have been developed to study the airflow in nasal cavities. However, several of these studies [3, 4] were performed using simplified or up-scaled models. This is mainly due to the challenge in segmenting the complex geometry of the nasal cavity from images acquired using computed tomography (CT) or magnetic resonance imaging (MRI). In [5], image slices were interpolated to increase the image data resolution and the airway is extracted using a region growing algorithm, while a thresholding method is used in [6] to extract the airway model. However, these methods may not be able to extract the nasal cavity accurately due to the complex and compact structure of the nasal cavity, and the noise and image inhomogeneity that exist in the dataset.

Deformable models are highly appropriate in segmenting these upper airway structures since they can naturally adapt to local image structures. However, explicit or parametric models are not suitable in our case since they generally have difficulties in dealing with topological changes and reaching into deep concavities and thin structures. Implicit deformable models based on the level set technique are introduced by Caselles et al. [7] and Malladi et al. [8] to address some of the limitations of parametric deformable models. In this approach, the evolution of curves and surfaces are represented implicitly as a level set of a higher-dimensional scalar function and the deformation of the model is based on geometric measures such as the unit normal and curvature. Thus, the evolution is independent of the parameterisation, and thus topological changes such as those in the complex geometry of the nasal cavity can be handled automatically.

In this paper, we draw our inspiration from the bidirectional and dynamic nature of the magnetostatic force used in the 2D magnetostatic active contour (MAC) model [9] to formulate a new external force field which is suitable for 3D image data. Briefly, the proposed deformable model uses an external force field that is based on the relative position and orientation of the deformable surface and object boundaries. This force field is called the *geometric potential force (GPF)* field as it is based on the hypothesised interactions between the relative geometries of the deforming surface and the image object boundaries (characterised by image gradients). The evolution of the deformable model is solved using the level set method. In this preliminary study, the new deformable model is applied to the segmentation of the complex structures of the human upper airway, including nasal cavity and sinuses, from a 3D CT image dataset.

2 Proposed Method

A deformable model is a sequence of contour or surface models obtained by taking an initial model and incrementally modifying its shape [10]. It provides an effective way to reconstruct continuous contours or surfaces from 2D or 3D data. Depending on the assumption of how an object boundary is described, deformable contour and surface models can be classified into image gradient based [8, 9, 11–13], region based [14, 15], and hybrid approaches [16, 17]. For image gradient based methods, it is assumed that object boundaries collocate with image intensity discontinuities which is widely adopted in various computer vision problems. Region based techniques, on the other hand, assume that object boundaries collocate with discontinuities in regional characteristics, such as colour and texture. In other words, each object has its own distinctive and continuous regional features, which is not always true for real world data, for example, due to intensity inhomogeneity and multi-modal nature. Conventional image gradient based methods have difficulties in dealing with image noise, weak edges and difficult initialisations as they are generally prone to local minima that can frequently appear in real images. Numerous research works have been reported in the literature to improve the gradient based approach. The balloon force [8] can effectively expand or shrink the contours, however, has great difficulties in handling weak edges and cross boundary initialisations. The bidirectionality of the gradient vector flow (GVF) model [11] allows more flexible initialisation and its diffused force field handles image noise interference in a much better manner. However, it has convergence issues caused by critical points in its force field [9, 12, 18]. More recent attempts, such as [12, 13, 18], showed promising but limited success.

In [9], Xie and Mirmehdi proposed a novel deformable contour model based on hypothesized magnetic interactions among gradient vectors and contours. This image gradient based method showed significant improvements on convergence issues, e.g. reaching deep concavities, and in handling weak edges and broken boundaries. While applying the analogy directly to deformable modelling it requires estimation of tangent vectors for the deformable contours, which is convenient in 2D case, however, not possible in 3D. In this paper, we introduce a hypothesized geometrically induced force field between the deformable model and object boundary that is based on the relative position and orientation of the geometries. In other words, the magnitude and direction of the interaction forces are based on the relative position and orientation between the geometries of the deformable model and the image object boundaries, and, hence, it is called the geometric potential force field. This new external force field is similar to the magnetic force field used on 2D images in MAC [9], but unlike [9], the proposed force field can be readily generalized to a higher dimension.

2.1 Formulation of the geometric potential force

As in [9], the external force field is based on the hypothesized magnetic force between the active contour and object boundaries. Consider two elements dl_1 and dl_2 of contours with currents I_1 and I_2, and tangent unit vectors $\hat{\boldsymbol{t}}_1$ and $\hat{\boldsymbol{t}}_2$, respectively. According to the Biot-Savart law, the magnetic flux density $d\boldsymbol{B}$ created by the element dl_1 and the corresponding force $d\boldsymbol{F}$ acting on dl_1 due to dl_2 are

$$\begin{cases} d\boldsymbol{B} = \dfrac{\mu_0}{4\pi}\dfrac{I_2 dl_2}{r^2}(\hat{\boldsymbol{t}}_2 \times \hat{\boldsymbol{r}}_{21}) \\ d\boldsymbol{F} = I_1 dl_1(\hat{\boldsymbol{t}}_1 \times d\boldsymbol{B}) \end{cases} \tag{1}$$

where r is the distance between dl_1 and dl_2, $\hat{\boldsymbol{r}}_{21}$ is the unit vector pointing from dl_2 to dl_1, and μ_0 is the permeability constant. Note the term $\mu_0/(4\pi)$ in (1) is a real constant, which can be ignored while adapting it to deformable modelling, i.e. $\mu_0/(4\pi) = 1$. This formulation has been applied directly in MAC [9] to compute the magnetic field and force required to draw the active contour towards object boundaries in 2D images. Note that the current directions represented by the tangent vectors $\hat{\boldsymbol{t}}_1$ and $\hat{\boldsymbol{t}}_2$ have to be known in advance before computing the magnetic field and force. To deal with this requirement, the authors in [9] compute the direction of the imposed currents for the active contour and object boundary by rotating the respective gradient vectors in a clockwise or anti-clockwise manner such that a current loop is formed on both the active contour and object boundary.

However, it is difficult to extend MAC to handle 3D images directly as it is not apparent how the hypothesized current direction is to be estimated and set on a 3D object. Here, we show how we can solve the problem of estimating the hypothesized current direction in [9], and show the formulation of the new geometric potential force field.

First, we re-write (1) the 2D problem in a slightly different manner allowing 3D generalization. Let vector $\hat{\boldsymbol{z}} = (0, 0, 1)$ be the normal to the plane where the active contour and object boundary are lying on. The tangent vectors on the length elements can now be represented as $\hat{\boldsymbol{t}}_1 = \hat{\boldsymbol{z}} \times \hat{\boldsymbol{n}}_1$ and $\hat{\boldsymbol{t}}_2 = \hat{\boldsymbol{z}} \times \hat{\boldsymbol{n}}_2$, where $\hat{\boldsymbol{n}}_1$ and $\hat{\boldsymbol{n}}_2$ are the unit normals to the contour and object boundary at dl_1 and dl_2 respectively (refer to Figure 1). The magnetic flux density created by dl_2 at

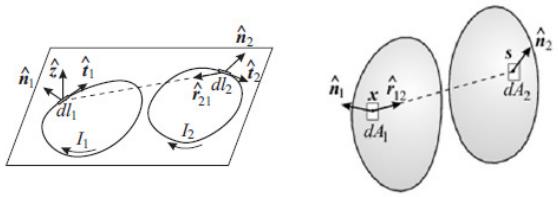

Figure 1. Relative position and orientation between geometries: left (2D contours) and right (3D surfaces).

dl_1 can now be written as

$$d\boldsymbol{B} = -\frac{I_2 dl_2}{r^2}(\hat{\boldsymbol{z}}\,(\hat{\boldsymbol{r}}_{21}\cdot\hat{\boldsymbol{n}}_2)) \tag{2}$$

Then the force acting on dl_1 by dl_2 can be given by a simple expression

$$\begin{cases} d\boldsymbol{F} &= -\dfrac{(I_1 dl_1)(I_2 dl_2)}{r^2}\,\hat{\boldsymbol{n}}_1(\hat{\boldsymbol{r}}_{21}\cdot\hat{\boldsymbol{n}}_2) \\ &= (I_1 dl_1\hat{\boldsymbol{n}}_1)\,dG \\ dG &= -\dfrac{I_2 dl_2}{r^2}\,(\hat{\boldsymbol{r}}_{21}\cdot\hat{\boldsymbol{n}}_2) \end{cases} \tag{3}$$

Note that the magnetic field in the 2D model has only a vertical component: $d\boldsymbol{B} = (0, 0, dG)$ and can be treated as a scalar dG. This formulation is analogous to the magnetic force field used on 2D images in [9], however, the new external force field has a different physical meaning compared to the traditional magnetic force field. In particular, one can look at the geometric potential dG as a induced scalar field, in which the strength of dG depends on the relative position of the two elements dl_1 and dl_2. The magnitude and direction of the geometrically induced vector force $d\boldsymbol{F}$ is therefore handled intrinsically by the relative position and orientation between the geometries of the deformable model and object boundary.

More importantly, this new force field can be easily extended to higher dimensions, and a generalized 3D version of the geometric potential force acting between two area elements dA_1 and dA_2 can be readily given as

$$\begin{cases} d\boldsymbol{F} = I_1 dA_1\hat{\boldsymbol{n}}_1 dG, \\ dG = \dfrac{I_2 dA_2}{r^3}(\hat{\boldsymbol{r}}_{12}\cdot\hat{\boldsymbol{n}}_2) \end{cases} \tag{4}$$

where dG the corresponding 3D potential field, and, obviously, $\hat{\boldsymbol{r}}_{12} = -\hat{\boldsymbol{r}}_{21}$. The exponent for r in (4) has been changed from 2 to 3 in order to maintain its physical meaning while extending from 2D to 3D.

2.2 Deformable model based on geometric potential force

Let the 3D image be described by function $u(\boldsymbol{x})$ where $\boldsymbol{x}$ is a pixel or voxel location in the image domain, and ∇u be its gradient. Let dA_1 belongs to the deformable surface with unit normal $\hat{\boldsymbol{n}}_1$ whereas dA_2 belongs to the object boundary with unit normal $\hat{\boldsymbol{n}}_2$. To compute the force acting on dA_1 from dA_2, we set I_1 as unity and substitute $I_2 = |\nabla u|$ and $\hat{\boldsymbol{n}}_2 = \nabla u/|\nabla u|$ into (4). Then we compute the total geometric potential field strength $G(\boldsymbol{x})$ at every voxel. Note that only voxels on the object boundary will contribute to the geometric interaction field. Let $\mathcal{S}$ denote the set containing all the edge voxels, and $\boldsymbol{s}$ denote a boundary voxel, the total geometric interaction at $\boldsymbol{x}$ can then be computed as:

$$G(\boldsymbol{x}) = P.V.\iint_{\mathcal{S}} \frac{\hat{\boldsymbol{r}}_{\boldsymbol{xs}}}{r^3_{\boldsymbol{xs}}}\cdot\hat{\boldsymbol{n}}_2(\boldsymbol{s})I_2(\boldsymbol{s})\,dA_{\boldsymbol{s}} \tag{5}$$

where $\hat{\boldsymbol{r}}_{\boldsymbol{xs}}$ is the unit vector from $\boldsymbol{x}$ to $\boldsymbol{s}$, and $r_{\boldsymbol{xs}}$ is the distance between them. Computation of (5) is efficiently carried out based on the 3D fast Fourier transform (FFT).

The force acting due to the geometrically induced potential field on the deformable surface $\mathcal{C}$ at the position $\boldsymbol{x} \in \mathcal{C}$ can then be given as:

$$\boldsymbol{F}(\boldsymbol{x}) = dA_{\boldsymbol{x}}\,\hat{\boldsymbol{n}}(\boldsymbol{x})\;G(\boldsymbol{x}) \tag{6}$$

Given the force field $\boldsymbol{F}(\boldsymbol{x})$ derived from the hypothesized interactions based on the relative geometries of the deformable model and object boundary, the evolution of the deformable model $C(\boldsymbol{x}, t)$ under this force field can be given

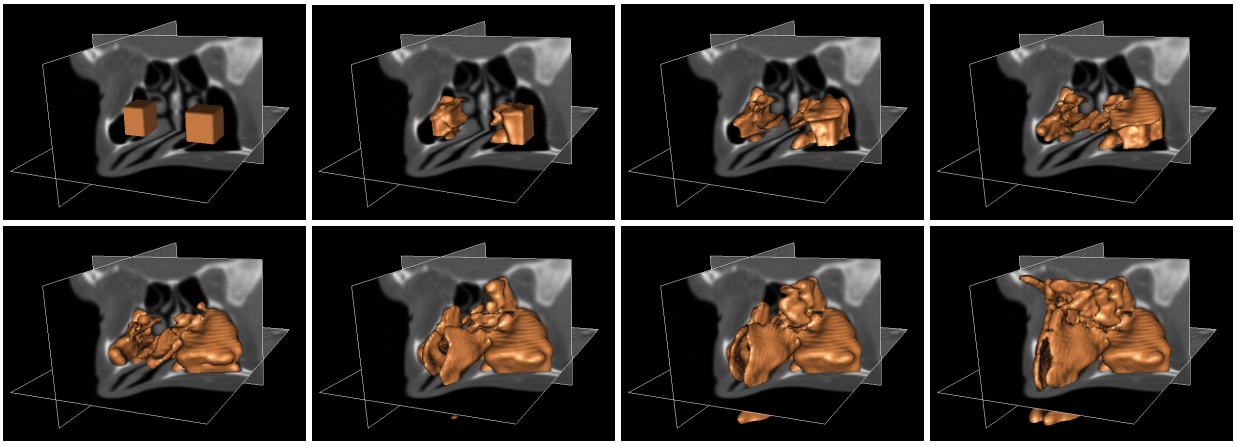

Figure 2. Segmentation of the human upper airway - from left to right, top to bottom: initial level set surface, intermediate stages of the level set evolution, and the converged deformable model.

as:

$$C_t = \left(\boldsymbol{F} \cdot \hat{\boldsymbol{n}}\right) \hat{\boldsymbol{n}} \tag{7}$$

Since contour or surface smoothing is usually desirable, the mean curvature flow is added and the complete geometric potential deformable model evolution can be formulated as:

$$C_t = \alpha g(\boldsymbol{x}) \kappa \hat{\boldsymbol{n}} + (1-\alpha)(\boldsymbol{F} \cdot \hat{\boldsymbol{n}}) \hat{\boldsymbol{n}} \tag{8}$$

where κ denotes the curvature, $g(\boldsymbol{x}) = \dfrac{1}{1+|\nabla u(\boldsymbol{x})|}$ is the edge stopping function, and α is a real constant to control the weight for smoothing. Its level set representation can then be given as:

$$\Phi_t = \alpha g \kappa |\nabla \Phi| - (1-\alpha)(\boldsymbol{F} \cdot |\nabla \Phi|) \tag{9}$$

3 Results

The new deformable model based on the geometrically induced force is applied in the segmentation of the human upper airway. The 3D image dataset of the human airway used for this experiment is acquired from CT imaging. The image dataset is then cropped to obtained the region containing the nasal cavity. This is done so as to reduce the computational expenses in using the level set method. A simple global thresholding is also applied to remove very bright regions. Those regions are known to be bone regions and often accompanied by high image gradient. Thus, this pre-processing can minimise their interference in segmenting the airway. Figure 2 portrays the results of the segmentation process using the proposed method. The different views of the segmented nasal cavity model is then shown in Figure 3.

As shown in the Figure 2, two initial level set surfaces are used for the segmentation process. In particular, the level set surfaces are being initialised across different structures (i.e. across object boundaries) in the image to demonstrate the capability of the new deformable model to deal with arbitrary cross-initialisations. The evolution process of the level set surface and the converged deformable model is also shown in the figure.

The example demonstrates that the proposed deformable model can be used to efficiently segment complex structures such as those of the human nasal cavity. Reasonable results were achieved without any dedicated initialisations. Note, this is an image gradient based method, i.e. only using local edge information. Further comparison to region based approaches on hand-labelled data is necessary. However, it is worth noting that it is not possible for other image gradient based approaches, such as geodesic [7], GVF [11], CVF [18] and GeoGVF [12], to achieve such result.

4 Discussion

In this paper, we presented a novel external force field for image segmentation which is based on hypothesized geometrically induced interactions between the deformable surface and the image object boundary. The proposed deformable model is then applied to segmenting human upper airway from a 3D image dataset. It is shown that by using this approach, complex geometries such as the nasal cavity can be efficiently reconstructed. Accordingly, the new external force is dynamic in nature as it changes according to the relative position and orientation between the evolving

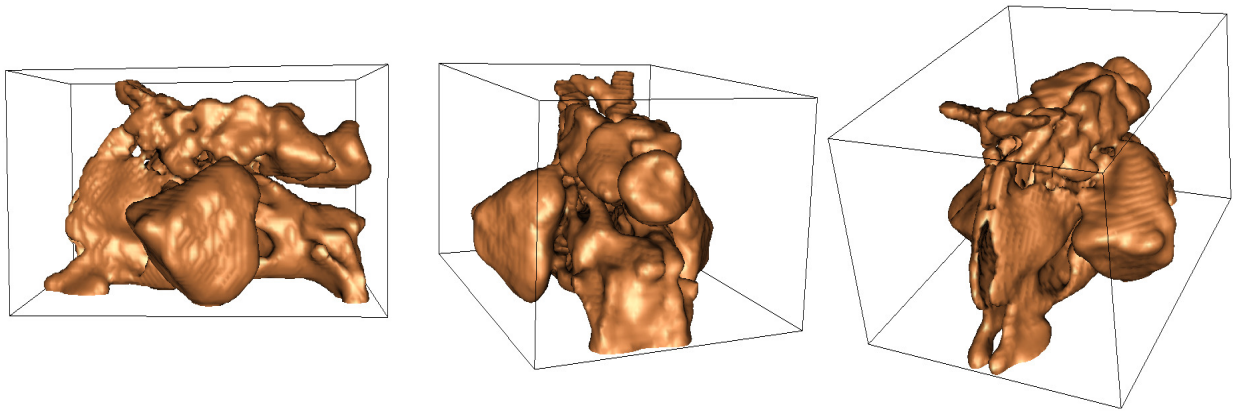

Figure 3. Three different views of the segmented human upper airway.

deformable model and object boundary. It can thus be used to attract the deformable model into deep boundary concavities that exists in some image objects. In addition, the new deformable model can handle arbitrary cross-initialisation which is a desirable feature to have, especially in the segmentation of complex and compact geometries. These are encouraging advantages compared to existing image gradient based deformable models. Quantitative analysis and comparison to region based methods are necessary to further study the performance of the proposed model. However, this preliminary work shows that this is a promising approach to reconstructing complex 3D objects and can provide an good alternative to region based methods, particularly when region based assumptions are compromised due to, for example, intensity inhomogeneity.

References

1. S. K. Kim & S. K. Chung. "An investigation on airflow in disordered nasal cavity and its corrected models by tomographic PIV." *Measurement Science and Technology* **15**, pp. 1090–1096, 2004.
2. J. Zhang, Y. Liu, X. Sun et al. "Computational fluid dynamics simulations of respiratory airflow in human nasal cavity and its characteristic dimension study." *Acta Mechanica Sinica* **24**, pp. 223–228, 2008.
3. M. Tarabichi & N. Fanous. "Finite element analysis of airflow in the nasal valve." *Otolaryngology Head and Neck Surgery* **119**, pp. 169–172, 1993.
4. D. Elad, R. Liebenthal, B. L. Wenig et al. "Analysis of air flow patterns in the human nose." *Medical and Biological Engineering and Computing* **31**, pp. 585–592, 1993.
5. K. Wang, T. S. Denney, E. E. Morrison et al. "Numerical simulation of air flow in the human nasal cavity." In *IEEE Engineering in Medicine and Biology*, pp. 5607–5610. 2005.
6. A. Y. T. Leung, W. S. Tsui, J. N. Xu et al. "Nasal airflow simulations in models derived from cone beam and spiral ct scans by using CFD." *J. Applied Mathematics and Mechanics* **3**, pp. 49–6, 2007.
7. V. Caselles, F. Catte, T. Coll et al. "A geometric model for active contours." *Numerische Mathematik* **66**, pp. 1–31, 1993.
8. R. Malladi, J. A. Sethian & B. C. Vemuri. "Shape modelling with front propagation: A level set approach." *IEEE Transations on Pattern Analysis and Machine Intelligence* **17(2)**, pp. 158–175, 1995.
9. X. Xie & M. Mirmehdi. "MAC: Magnetostatic active contour model." *IEEE Transations on Pattern Analysis and Machine Intelligence* **30(4)**, pp. 632–647, 2008.
10. R. Whitaker. "Modeling deformable surfaces with level sets." *IEEE Computer Graphics and Applications* **24(5)**, pp. 6–9, 2004.
11. C. Xu & J. L. Prince. "Snakes, shapes, and gradient vector flow." *IEEE Transactions on Image Processing* **7(3)**, pp. 359–369, 1998.
12. N. Paragios, O. Mellina-Gottardo & V. Ramesh. "Gradient vector flow geometric active contours." *IEEE Transations on Pattern Analysis and Machine Intelligence* **26(3)**, pp. 402–407, 2004.
13. C. Li, J. Liu & M. Fox. "Segmentation of edge preserving gradient vector flow: an approach toward automatically initializing and splitting of snakes." In *IEEE Conference on Computer Vision Pattern Recognition*, pp. 162–167. 2005.
14. A. Farag & H. Hassan. "Adaptive segmentation of multi-modal 3D data using robust level set techniques." In *Medical Image Computing and Computer-Assisted Intervention*, pp. 143–150. 2004.
15. D. Cremers, M. Rousson & R. Deriche. "A review of statistical approaches to level set segmentation: Integrating color, texture, motion and shape." *International Journal of Computer Vision* **72(2)**, pp. 195–215, 2007.
16. A. Chakraborty, H. Staib & J. Duncan. "Deformable boundary finding in medical images by integrating gradient and region information." *IEEE Transactions on Medical Imaging* **15(6)**, pp. 859–870, 1996.
17. X. Xie & M. Mirmehdi. "RAGS: Region-aided geometric snake." *IEEE Transactions on Image Processing* **13(5)**, pp. 640–652, 2004.
18. D. Gil & P. Radeva. "Curvature vector flow to assure convergent deformable models for shape modelling." In *Energy Minimization Methods in Computer Vision and Pattern Recognition*, pp. 357–372. 2003.